A Method for Identifying Tubercle Bacilli using Neural Networks

Sheng-Fuu Lin, Hsien-Tse Chen

Department of Electrical and Control Engineering
National Chiao Tung University, Taiwan 30010, Republic of China
(Received September 4, 2008. Accepted May 13, 2009)

Abstract

Phlegm smear testing for acid-fast bacilli (AFB) requires careful examination of tubercle bacilli under a microscope to distinguish between positive and negative findings. The biggest weakness of this method is the visual limitations of the examiners. It is also time-consuming, and mistakes may easily occur. This paper proposes a method of identifying tubercle bacilli that uses a computer instead of a human. To address the challenges of AFB testing, this study designs and investigates image systems that can be used to identify tubercle bacilli. The proposed system uses an electronic microscope to capture digital images that are then processed through feature extraction, image segmentation, image recognition, and neural networks to analyze tubercle bacilli. The proposed system can detect the amount of tubercle bacilli and find their locations. This paper analyzes 184 tubercle bacilli images. Fifty images are used to train the artificial neural network, and the rest are used for testing. The proposed system has a 95.6% successful identification rate, and only takes 0.8 seconds to identify an image.

Key words : Tubercle bacilli, digital image processing, feature extraction, neural network.

I. INTRODUCTION

Testing for acid-fast bacilli (AFB) often requires a lot of time and manpower to read a slide with phlegm using merely naked eyes and a microscope. Generally speaking, this process is time consuming and exhausting, and is therefore likely to produce incorrect results. To reduce these errors and increase analysis efficiency, this study proposes image technology and identification methods to count tubercle bacilli [1].

This paper uses digital imaging to identify and count tubercle bacilli on a slide under a microscope using automatic image processing and pattern recognition. This paper focuses on the Ziehl-Neelsen's [2] method of analyzing AFB. Ziehl-Neelsen's [2] method is a special bacteriological stain used to identify acid-fast organisms, especially Mycobacteria. Tubercle bacilli are the most important part of organisms. This approach makes it easier to find tubercle bacilli since their lipid rich cell walls make them resistant to Gram stain. Ziehl-Neelsen's [2] method can also be used to stain other bacteria, such as Nocardia. If we apply it to medical clinical science, we do not need to analyze all images. Generally speaking, there are 300 images on a slide. This approach only requires a few images (9 or more tubercle bacilli in an image) to determine whether or not a patient suffers from tuberculosis (see Table 1). This reduces the manpower and time required to correctly diagnose a patient with tuberculosis.

Foreroa [1] applied a technique of counting color steps to fluorescence micrograph. Otsu's [3] method which selects a threshold automatically from a gray level histogram was derived from discriminant analysis. Otsu's [3] method directly deals with evaluating the goodness of thresholds, and the optimal threshold (or set of thresholds) is selected by the discriminant criterion. Liu's [4] proposed Shape Model-Based technique for cutting blood cells.

Corresponding Author : Sheng-Fuu Lin
Department of Electrical and Control Engineering, National Chiao Tung University
1001 Ta-Hsueh Road, Hsinchu 30010, Taiwan, Republic of China
Tel : 886-3-571-2121 / Fxt : 886-3-571-5998
Email : sflin@mail.nctu.edu.tw; hsientse.ece93g@nctu.edu.tw
This paper is based on the deeply appreciated support by Dr.Tung-Lung Tsai in Otorhinolaryngology-Head and Neck Surgery Taipei Veterans General Hospital, assisting in acquiring the images of tubercle bacilli. This work was supported partially by the National Science Council under Grant NSC 96-2221-E-009-238.

II. MATERIALS AND METHODS

The proposed method can be divided into three phases with the following steps (see Figure 1). First, segment the image and collect the characteristics of the segmented images. Second, segment the images, categorize them based on the length, roundness, and area of the tubercle bacilli. Third, classify them by the type of neural network which will be used

Table 1. The Method of AFB Originates from the reference [2].

Quantity of tubercle bacilli observed under the oil mirror	Reported results
None	No AFB observed
1-2/300 fields	+/-
1-9/100 fields	1+
1-9/10 fields	2+
1-9/ fields	3+
>9/fields	4+

If it is <3/300 fields should be examined again or made a new slice to confirm when the oil mirror is examined.

to train them, and then perform that training of the neural network based on the form and characteristics of the tubercle bacilli. Next, divide the remaining test materials into single tubercle bacilli, non-tubercle bacilli, and overlapping tubercle bacilli. It is then possible to calculate the corresponding quantity of tubercle bacilli by classifying the images into different types of neural networks.

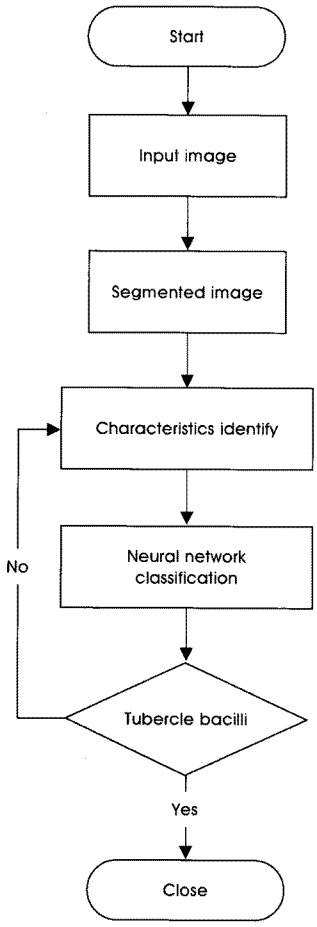

Fig. 1. System flow chart.

The experiments in this study used a microscope eyepiece with 10x magnification and an objective magnification of 100x. A digital camera or Charge Coupled Device (CCD) was placed on the microscope eyepiece to take digital images of tubercle bacilli for analysis. The digital camera used in this study had a horizontal and vertical resolution of 150 dot per inch (dpi). Each image is 1388 pixels wide and 1040 pixels tall, with 24-bit color imaging.

A. Image Segmentation

To receive the characteristic value of the tubercle bacilli, it is necessary to segment the image. This image after segmentation is a binary image. The purpose of segmentation is to separate the tubercle bacilli from background impurities. This study uses the Otsu [3] automatic best value searching algorithm and color information to carry out segmentation. Otsu utilized statistical analysis to identify the method that yields the within-class minimum of every group and the critical value of the between-class maximum. This approach enables a tubercle bacilli cell's image to be separated from the background [5, 8].

However, the Otsu algorithm may be affected by noise on a slide when fetching a tubercle bacilli image. This makes it difficult to separate the tubercle bacilli from the background, and may produce inadequate binary results. Therefore, this study also uses color information to strengthen the results of binary segmentation (see Figure 2).

Although the Otsu algorithm can probably still find tubercle bacillus, it may require an excessive amount of searching time if the background is too complicated. To address this problem, this study uses a hue of hue, intensity and saturation (HIS) in color space to dye the tubercle bacillus and perform color analysis (see Figure 3). Hue can be defined as below :

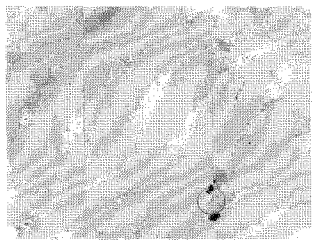

(a) (b)

Fig. 2. The compare with original image and segment by Otsu's method of automatic threshold selection: (a) original image (enclose red is tubercle bacillus and hand sketch) and (b) segment by Otsu's method of automatic threshold selection.

$$H = \begin{cases} \theta & \text{if } B \leq G \\ 360 - \theta & \text{if } B > G \end{cases}$$

where

$$\theta = \cos^{-1}\left\{ \frac{\frac{1}{2}[(R-G)+(R-B)]}{[(R-G)^2+(R-B)(G-B)]^{1/2}} \right\} \quad (1)$$

Experiment results show that a difference between the R value and the G value, and this difference increases when there are tubercle bacillus in the image. The H value also increases in this case, but the B value does not change (see Figure 4).

The proposed image segmentation method first applies the Otsu algorithm to find the probable tubercle bacilli. The next step is to utilize these tubercle bacilli to determine the difference between the R value and the G value, and then use H value to calculate quantitative value (see equation 2). This process accurately identifies tubercle bacilli.

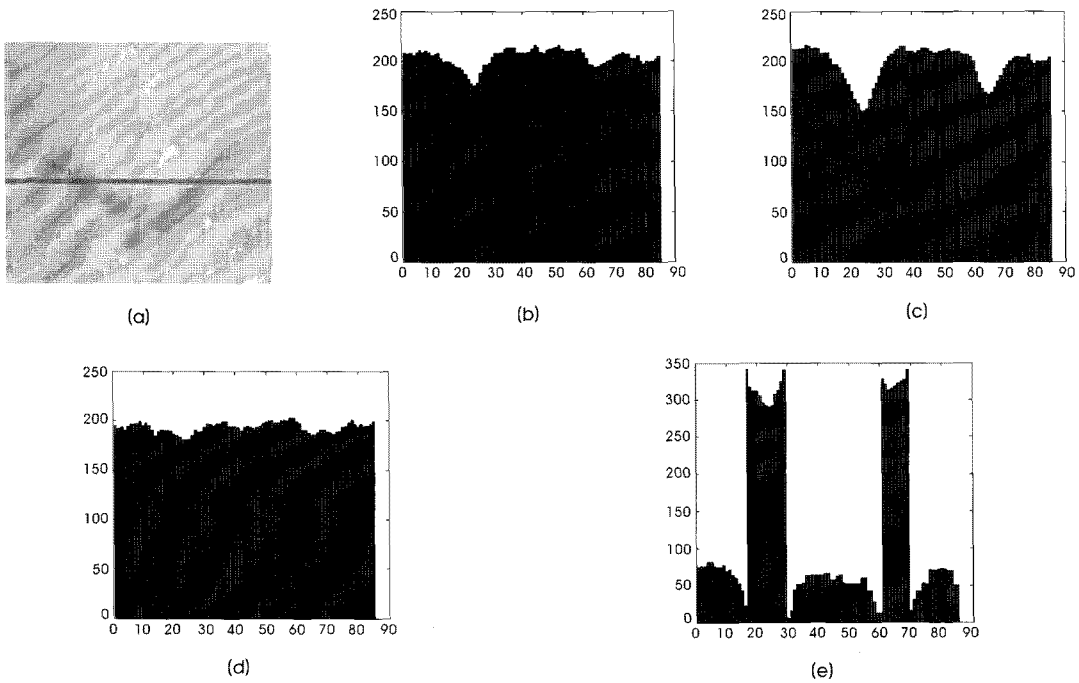

Fig. 3. Example of a region that contains an isolated bacillus: (a) real image (red line is hand sketch), (b) histogram of R, (c) histogram of G, (d) histogram of B and (e) histogram of H.

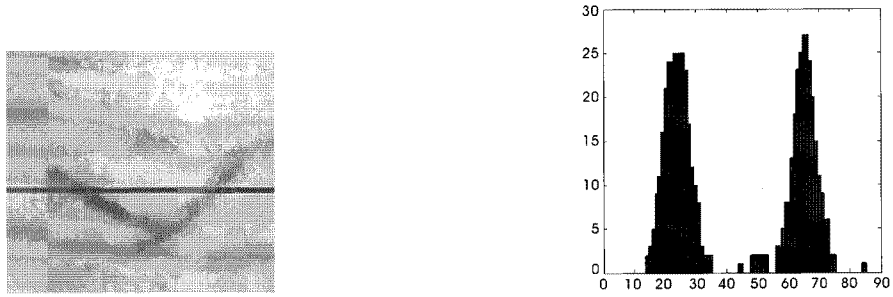

Fig. 4. Example of a region that contains an isolated bacillus: (a) real image (red line is hand sketch) and (b) histogram of R-H.

$$\begin{aligned} R-G &> 10, \\ H &> 260, \\ B &\cong 200, \end{aligned} \tag{2}$$

Even after roughly highlighting the tubercle bacilli, fracturing of the highlighted tubercle bacilli or discontinuity may occur because the dye on the slide may be stained or faded. Therefore, this study uses a morphology closing filter to repair fractured parts of a cell [4-6].

B. Feature Extraction

The most realistic method of differentiating between true tubercle bacillus and excessive dyeing tubercle bacillus is to extract the eigenvalue of real tubercle bacillus. First, refer to the examination results; the tubercle bacillus has a light red, bar shaped appearance, and is aligned in various directions. Then, digitize these tubercle bacilli features and make the computer identify tubercle bacillus (see Table 2).

Table 2 shows the method of determining tubercle bacillus based on existing medical experience. This method focuses on extracting and calculating the forms and features of tubercle bacillus, including length, roundness, Hu's invariant moment, area, and perimeter. These parameters are regarded as training type neural parameters, as follows:

1. Area (A): the total number of pixels in the target area.
2. Perimeter (P): the total number of pixels from any point to the tubercle bacilli along an edge in the target area.
3. Roundness (R): this value ranges between 1 and 0. The rounder the body is, the closer the roundness is to 1.

$$R = \frac{4\pi A}{(P)^2} \tag{3}$$

4. Length: the longest route after the target area is thinned.
5. All length: the total length of all routes after the target area is thinned.
6. Invariant moment (hu_1) [7]: the tubercle bacilli in this study always have the same form, but with different angles and sizes. Thus, the invariant moment is included as an extracted feature to utilize the fact that the invariant moment does not change with the variation, translation, rotation, and size of an image.

We can deduce seven invariant moments as follows:

$$\begin{aligned}
\phi_1 &= \eta_{20} + \eta_{02} \\
\phi_2 &= (\eta_{20} - \eta_{02})^2 + 4\eta_{11}^2 \\
\phi_3 &= (\eta_{30} - 3\eta_{12})^2 + (3\eta_{21} - \eta_{03})^2 \\
\phi_4 &= (\eta_{30} + \eta_{12})^2 + (\eta_{21} + \eta_{03})^2 \\
\phi_5 &= (\eta_{30} - 3\eta_{12})(\eta_{30} + \eta_{12})[(\eta_{30} + \eta_{12})^2 - 3(\eta_{21} + \eta_{03})^2] \\
&\quad + (3\eta_{21} - \eta_{03})(\eta_{21} + \eta_{03})[3(\eta_{30} + \eta_{12}) - (\eta_{21} + \eta_{03})^2] \\
\phi_6 &= (\eta_{20} - \eta_{02})[(\eta_{30} + \eta_{12})^2 - (\eta_{21} + \eta_{03})^2] \\
&\quad + 4\eta_{11}(\eta_{30} + \eta_{12})(\eta_{21} + \eta_{03}) \\
\phi_7 &= (3\eta_{21} - \eta_{03})(\eta_{30} + \eta_{12})[(\eta_{30} + \eta_{12})^2 - 3(\eta_{21} + \eta_{03})^2] \\
&\quad + (3\eta_{21} - \eta_{03})(\eta_{21} + \eta_{03})[3(\eta_{30} + \eta_{12}) - (\eta_{21} + \eta_{03})^2]
\end{aligned} \tag{4}$$

Table 2. Digitized features of the tubercle bacilli as determined by computer

Artificial decisions from examiner	Computer decisions
Light red	Otsu algorithm and color analysis
Rectangular shape	Analysis based on shape features such as length, roundness, and perimeter
Random direction	Analysis based on shape features (Hu's moment)

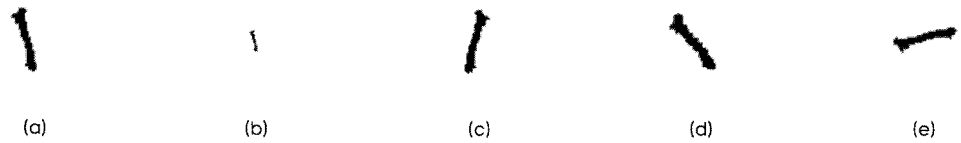

Fig. 5. (a) Original tubercle bacillus image, (b) narrow by half, (c) shine upon, (d) 45 degrees of clockwise rotations and (e) 90 degrees of clockwise rotations.

The invariant moment is not affected by translation; rotation and size (see Figure 5 and Table 3). Equation 4 shows that its output values will be very large. Because the logarithm function is an increasing function, this study uses the follo-wing equations instead of equation 4.

$$hu_i|\log(|\phi_i|)|,\ i = 1,\ 2,\ ...,\ 7 \tag{5}$$

In all these equations, ϕ_i is the value of the invariant moment after calculation.

The directions and sizes of most tubercle bacilli are similar, and only the directions of single tubercle bacilli are different. Thus, we can utilize the fact that the invariant moment does not change with variations in angle and size to identify real tubercle bacilli. There is a fixed area within each tubercle bacilli. If the area of the eigenvalue exceeds the maximal area range, the object is a overlapping tubercle bacilli. However, because an excessively dyed area can only be the same as the area of single tubercle bacilli, this study does not treat excessive dyeing as overlapping tubercle bacilli.

C. Neural Networks and Counting

Since seven invariant moments share the characteristic of not being affected by shifting and whirling, this study designs neural networks [9-12] as three inputs and three outputs (see Figure 6. This study utilizes the three outputs as categorized results to determine the quantity of tubercle bacilli and determine the number of tubercle bacilli in a digital image.

Figure 5 shows the proposed back transmission neural network model. The input 3×1 vector is length, all length, and invariant moment's first equation $|\log(|\phi_1|)|$ respectively. The output 3×1 vector is single tubercle bacillus, non-tubercle bacilli, and overlapping tubercle bacilli, respectively. There are three dimensioning input vectors and three dimension output vectors. The three output vectors are (1,0,0), (0,1,0), and (0,0,1), which respectively represent single tubercle bacillus, non-tubercle bacilli, and overlapping tubercle bacilli (more than two tubercle bacilli). The learning process of the back transmission algorithm includes positive and negative spreads. In the positive spread process, input information weights operation from the input layer via hidden layers, transfers input information through activation function, and spreads to the output layer to calculate network exporting value. Each neuron layer only affects the state of the next neuron layer. If a neuron layer cannot receive the target value, it will transfer to the back transmission value and pass the error signal back along the original connection path. By revising the weight of every neuron layer, this study hopes to stop errors within the tolerated error range.

$IW\{1, 1\}$ is the input weight matrix of 15×3, its input is a

Table 3. Invariant moment value of Figure 5

Invariant moment	original image	narrow by half	shine upon	45 degrees of clockwise rotations	90 degrees of clockwise rotations
$\|\log(\|\phi_1\|)\|$	1.9925	1.9872	1.9862	1.9745	1.9984
$\|\log(\|\phi_2\|)\|$	3.8500	3.8725	3.8658	3.8125	3.8954
$\|\log(\|\phi_3\|)\|$	2.4795	2.5712	2.5124	2.5475	2.4618
$\|\log(\|\phi_4\|)\|$	2.6820	2.6321	2.6748	2.6125	2.6344
$\|\log(\|\phi_5\|)\|$	5.4210	5.3219	5.3965	5.3478	5.4197
$\|\log(\|\phi_6\|)\|$	4.6421	4.5810	4.5745	4.5630	4.6465
$\|\log(\|\phi_7\|)\|$	5.3287	5.3679	5.3159	5.3128	5.3074

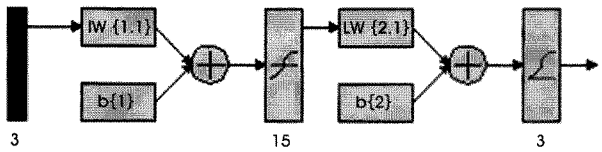

Fig. 6. Back propagation neural network.

vector quantity of 3×1, and $b(1)$ is the biased weight vector of 15×1. The equation 5 is the function of middle hidden layer. Middle hidden layer input is the vector of 15×1. The activation function in the middle of the hidden layer is a tangent double crooked function:

$$\frac{e^{n}-e^{-n}}{e^{n}+e^{-n}} \tag{6}$$

$LW\{2,1\}$ is the layer of the weight matrix of 3×15. Its input is a vector quantity of 15×1, and b (2) is the biased weight vector of 3×1. The equation 6 is the function of output layer. Output layer input is the vector of 3×1. The activation function in the output layer is a logarithm double crooked function:

$$\frac{1}{1+e^{-n}} \tag{7}$$

If a neural network is to operate correctly, the neural network must be continuously trained until it can accurately produce the necessary outputs. The samples necessary for training should be prepared in advance of each input to a neural network. The more numerous, accurate, and different the samples are, the stronger the ability of the neural network is. This study selected 50 digital images as training samples, and each image contained a different number of tubercle bacilli. Some images did not contain tubercle bacilli, while others contained more than 50. length, all length, and invariant moment's first equation $|\log(|\phi_1|)|$ features were extracted from each tubercle bacilli in these 50 digital images individually. The neural network then calculated the final weight output value after training. Finally, the remaining digital images were tested with these weight values.

Figure 6 shows an easy test of random fetches from 10 digital images. The disparity between the outputs and the ideal target decreases as the training increases. After 150 training iterations, the disparity does not change anymore. Specifically, the disparity reached 0.00042736 after 150 times of training. This is quite close to the target disparity of 0 in this study.

The remaining untrained samples can be tested after training the neural network. The total number of tubercle bacilli in 184 digital images after recounting includes single tubercle bacillus, not tubercle bacilli, and overlapping tubercle bacilli. These digital images are grouped according to the number of the tubercle bacilli, a small amount, middle

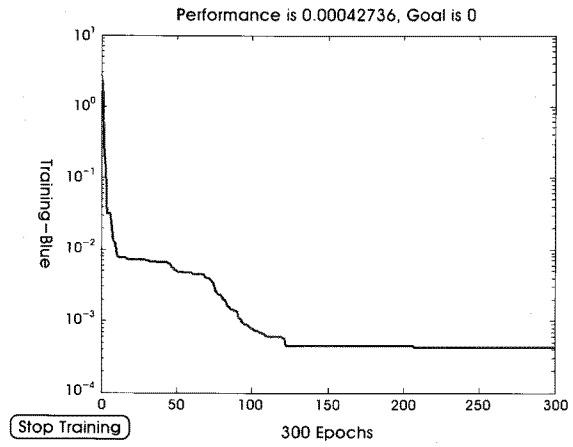

Fig. 7. 10 digits image trains and outputs pursuing with the ideal goal disparity relation.

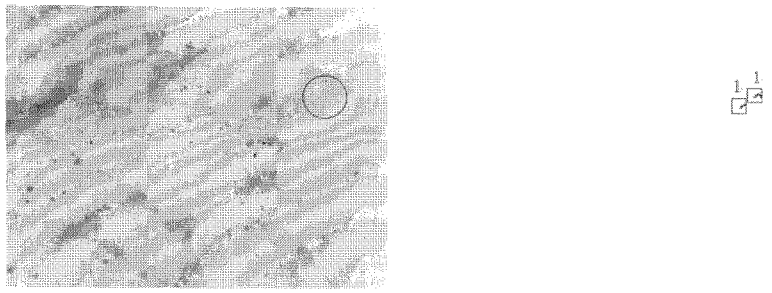

(a) (b)

Fig. 8. (a) The original image includes 2 tubercle bacilli (red circle by hand indicates tubercle bacilli) and (b) the system judges 2 tubercle bacilli.

amount, or a large amount of bacilli. A small amount of tubercle bacilli represents 0~2 tubercle bacilli, a middle amount of tubercle bacilli represents 3~9 tubercle bacilli, and a large amount of tubercle bacilli represents more than 9 tubercle bacilli. As for overlap, this study roughly estimates and examines overlap by the area of tubercle bacilli. This is because the area of overlapping tubercle bacilli can be reasonable estimated based on artificial experience when tubercle bacilli overlap. This assessment does not influence the final results. Table 1 show that medical science categorizes tubercle bacilli into 5 levels. As long as the number of tubercle bacilli in each image does not differ too much, the estimated findings will be the same as the artificial count.

Ⅲ. RESULTS AND DISCUSSION

This paper examines a total of 184 tubercle bacilli images. Fifty images are used to create a neural network, and the rest are used for testing. The proposed system has a 95.6 percent successful identification rate, and only takes 0.8 seconds to identify an image.

According to Table 1, the number of tubercle bacilli in each image is different. However, it is not necessary to refer to the total number of bacilli in the image. Instead, we can distinguish which kind of degree each slide belongs to based on how many tubercle bacilli it contains. Oother digital images must also be used to determine under what circumstances the little bacilli are to be counted. Thus, the digital images for testing are divided into three types, according to the number of the tubercle bacilli they contain: a small amount, middle amount, or a large amount of bacilli. A small amount of tubercle bacilli represents 0~2 tubercle bacilli, a middle amount of tubercle bacilli represents 3~9 tubercle bacilli, and a large amount of tubercle bacilli represents more than 9 tubercle bacilli. This study analyzes and deals with these three types of images individually.

First experiment group: The image includes 2 tubercle bacilli (see Figure 8).

Second experiment group: The image includes 7 tubercle bacilli (see Figure 9).

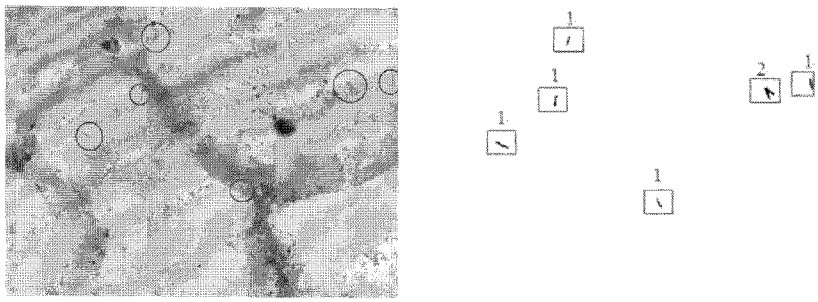

(a) (b)

Fig. 9. (a) The original image includes 7 tubercle bacilli (red circle by hand indicates tubercle bacilli) and (b) the system judges 7 tubercle bacilli.

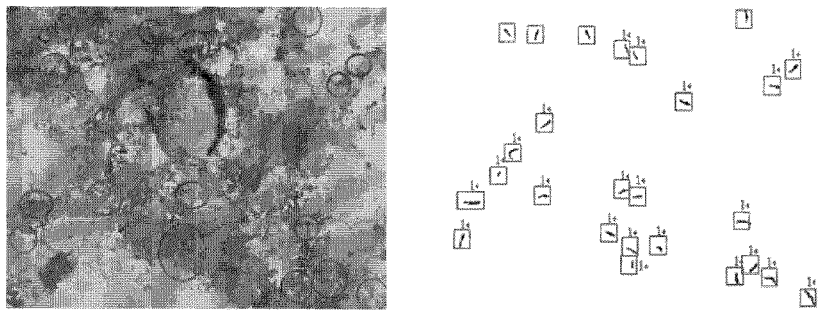

(a) (b)

Fig. 10. (a) The original image includes 28 tubercle bacilli (red circle by hand indicates tubercle bacilli) and (b) the system judges 26 tubercle bacilli.

Third experiment group: The image includes 28 tubercle bacilli (see Figure 10).

If we apply the proposed system to Table 1, the result will be the same as the result after an artificial count. There are three reasons for possible errors in this system's analysis. First, there may be too much impurity, which has piled up to the dyed tubercle bacilli. Second, this method identifies overlapping tubercle bacilli by the area of the tubercle bacilli. Although the overlapping tubercle bacilli are surely in the regular range of the area, they are often estimated with the naked eye. If the overlapping of tubercle bacilli is too complicated, tubercle bacilli will probably miss some of them (see Figure 10). Third, the tubercle bacilli may be blurred if the phlegm is daubed unevenly on the slide.

Ⅳ. CONCLUSIONS

This paper proposes a method that uses a computer, instead of manpower, to identify tubercle bacilli. The analysis of tubercle bacilli is time consuming, and has previously required a human examiner to avoid errors. Image processing techniques provide a good way to improve the manual screening of tubercle bacilli samples. At present, examiners still estimate the number of tubercle bacilli under a microscope using their naked eyes. This paper first obtains digital images with an electron microscope and then processes them with Otsu [2] algorithms. This approach can identify the tubercle bacilli from images alone. A neural network provides this technique with a 95.6 percent successful identification rate. Counting tubercle bacilli with a microscope and naked eyes requires about 1 to 2 seconds before. At present, it takes a computer only 0.8 seconds to perform the same task using the proposed method. This not only saves time, but also increases the efficiency of the examiner. This paper proves that computers can replace humans in identifying tubercle bacilli.

REFERENCES

[1] M. G. Forero, F. Sroubek, and G. Cristobal, "Identification of tuberculosis bacteria based on shape and color," *Real-Time Imaging*, vol. 10, no. 4, pp. 251-262, 2004.

[2] http://en.wikipedia.org/wiki/Ziehl-Neelsen_stain.

[3] N. Otsu, "A threshold selection method from gray-level histogram," *IEEE Trans. on Systems, Man and Cybernetics*, vol. 9, no. 1, pp. 62-66, 1979.

[4] L. Liu and S. Sclaroff, "Medical image segmentation and retrieval via deformable models," *Proc. IEEE Int. Conf. on Image Processing*, vol. 3, pp. 1071-1074, 2001.

[5] K. A. Marghani, S. S. Dlay, B. S. Sharif, and A. J. Sims, "Automated morphological analysis approach for classifying colorectal microscopic images," *Proc. of SPIE*, vol. 5267, pp. 249-249, 2003.

[6] F. Ortiz, F. Torres, E. D. Juan, and N. Cuenca, "Colour mathematical morphology for neural image analysis", *Real-Time Imaging*, vol. 8, pp. 455-465, 2002.

[7] K. Wu, D. Gauthier, and M. D. Levine, "Live Cell Image Segmentation," *IEEE Trans. on Biomedical Engineering*, vol. 42, pp. 1-12, 1995.

[8] J. R. Weaver and J. L Au, "Application of automatic thresholding in image analysis scoring of cells in human solid tumors labeled for proliferation markers," *Cytometry A*, vol. 29, pp. 128-135, 1997.

[9] S. F. Lin and C. A. Hung, *Introduction of Neural Networks and Pattern Recognition*. Taiwan: OpenTech, 2002(In Chinese).

[10] Z. F. Zhang, L. C. Zhang, and H. L. Huang. *Neural Network*. Taiwan: OpenTech, 2003 (In Chinese).

[11] R. Grzeszczuk, D. Terzopoulos, and G. Hinton, *NeuroAnimator: Fast Neural Network Emulation and Control of Physics-Based Models*. New York, ACM, 1998.

[12] Q. Zheng, B. K. Milthorpe, and A. S. Jones, "Direct neural network application for automated cell recognition," *Cytometry A*, vol. 57, pp. 1-9, 2004.